The 2012 World Congress on
Advances in Civil, Environmental, and Materials Research (ACEM' 12)
Seoul, Korea, August 26-30, 2012

Effect of the Wake of the Transducer Supports on the Ultrasonic Anemometer Measurements

*Sebastián Franchini[1)], Álvaro Cuerva[2)] and Angel Sanz-Andrés[3)]

IDR/UPM, E.T.S.I. Aeronáuticos, Universidad Politécnica de Madrid, E-28040 Madrid, Spain
[1)] s.franchini@upm.es

ABSTRACT

The wake produced by the structural supports of the ultrasonic anemometers (UAs) causes distortions in the velocity field in the vicinity of the sonic path. These distortions are measured by the UA, inducing errors in the determination of the mean velocity, turbulence intensity, spectrum, etc.; basic parameters to determine the effect of wind on structures. Additionally, these distortions can lead to indefinition in the calibration function of the sensors (Cuerva et al., 2004). Several wind tunnel tests have been dedicated to obtaining experimental data, from which have been developed fit models to describe and to correct these distortions (Kaimal, 1978 and Wyngaard, 1985).

This work explores the effect of a vortex wake generated by the supports of an UA, on the measurement of wind speed done by this instrument. To do this, the Von Karman´s vortex street potential model is combined with the mathematical model of the measuring process carried out by UAs developed by Franchini et al. (2007). The obtained results are the correction functions of the measured wind velocity, which depends on the geometry of the sonic anemometer and aerodynamic conditions.

These results have been validated with the ones obtained in a wind tunnel test done on a single path UA, especially developed for research. The supports of this UA have been modified in order to reproduce the conditions of the theoretical model. Good agreements between experimental and theoretical results have been found.

1. INTRODUCTION

Ultrasonic anemometry is a technique that measures the wind speed vector based on the detection of the influence of the flow field on the transmission of ultrasonic signals between a transmitter and a receiver. A pair of facing transducers defines a measurement path, which is able to measure the velocity vector component along it. The simplest configuration of a measurement path placed inside a uniform parallel flow, u_∞, is shown in Fig. 1. The transducers are placed facing each other and separated a distance l.

Most often, the supports of these sensors are tubes of circular cross section, with about 5×10^{-3} m diameter, as shown in Fig. 2, where some types of configurations of commercial anemometers are displayed. When placed exposed to an incoming flow, these cylindrical tubes produce wakes, which modifies the velocity field along the measurement path, therefore distorting the velocity measurements. In a typical wind speed range $1 < u_\infty < 20$ m/s the associated Reynolds number varies in the range

[1), 2), 3)] Ph.D.

$400 < Re < 7x10^3$. Fortunately, in this range there are mathematical models that describe in a very satisfactory way the velocity field in the wake produced by a cylindrical tube.

The aim of this paper is to determine the wake parameters that affect the speed measurement, and quantify the deviation of measurements produced by the distortion of the flow due to the wake. The approach followed is the application of the conclusions of a mathematical model presented in (Franchini 2007), and taking into account the velocity field that describes the wake. As a model of the wake, the so-called von Karman´s vortex street is considered.

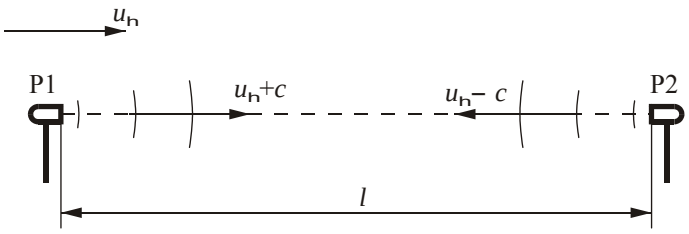

Fig. 1. The simplest configuration of a measurement path of length l, placed inside a uniform parallel flow, u_∞. P1 and P2 are the ultrasonic transducers and c is the sound speed.

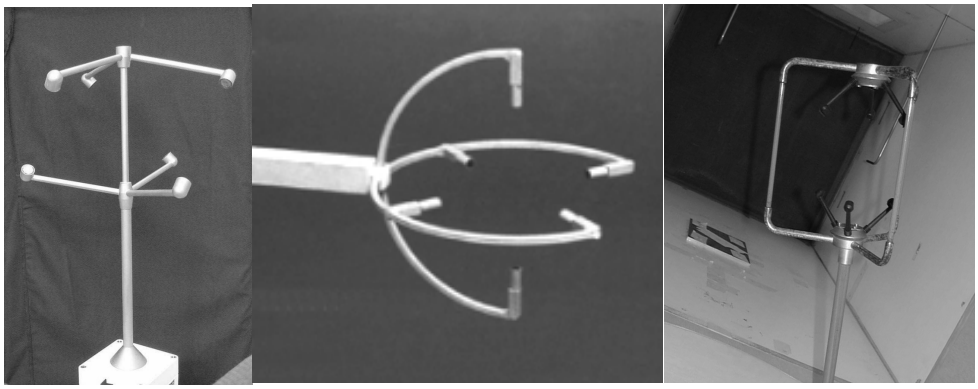

Fig. 2. Three-velocity components ultrasonic anemometer models. Metek 1-USA, Vx-Applied Technology, Windmaster-Gill Instruments (from left to right).

2. ULTRASONIC ANEMOMETER MEASUREMENT PROCESS

A detailed presentation of the problem can be found in (Franchini 2007); therefore, just a reduced summary is included here. Let us consider the trajectory travelled by an acoustic signal from the emitter, P1 to the receiver, P2, which depends on the velocity field present along the trajectory, as shown in Fig. 1.

Each transducer emits an ultrasound signal that travels towards the opposite transducer. The speed of propagation of the signals is the vector sum of the speed of sound in the media, c, and the local flow velocity vector along the measurement path. Therefore, the flow velocity field has a different effect on the propagation of signals in

each direction. From the measurement of the differences between the forward and backward transit times (t_+ and t_- respectively), the wind speed component along the measurement path can be obtained as:

$$u_M = \frac{l}{2}\left(\frac{1}{t_+} - \frac{1}{t_-}\right). \tag{1}$$

This is the inverse time algorithm, and it is used by most ultrasonic anemometers nowadays.

For the following analysis, the trajectory of the ultrasound pulse is considered to be included in *x, z* plane defined by two vectors: the direction of the measurement path (P1-P2) and the mean wind speed vector. It is assumed that the speed normal to this plane is negligible (or at least its mean value is zero). The time-of-flight measurement starts when the acoustic pulse is emitted by the transducer P1 and is finished when the transducer placed at P2 detects the first wave that arrives at it. Therefore, the problem consists in the determination of the minimum time-of-flight trajectory between P1 and P2, which is the trajectory that minimizes the value of the integral

$$t_+ = \int_{x_1}^{x_2} \frac{dx}{u_P(x,z,t)} \tag{2}$$

where t_+ is the time-of-flight of the acoustic pulse from P1 to P2 and $u_P(x,z,t)$ is the total velocity component of the acoustic pulse along *x*-axis. Using dimensionless variables

$$T_+ = t_+ \frac{c}{l}, \quad T_- = t_- \frac{c}{l}, \quad U = \frac{u_P}{u_\infty}, \tag{3}$$

where u_∞ is a reference velocity and, considering that the propagation of the acoustic pulse is a straight line, the dimensionless times-of-flight in the forward and backward directions, T_+ and T_-, are,

$$T_+ = 1 - \overline{U_0} M + O(M^2), \tag{4}$$

$$T_- = 1 + \overline{U_0} M + O(M^2), \tag{5}$$

where $M = u_\infty/c$ is the Mach number and

$$\overline{U_0} = \int_{-\frac{1}{2}}^{\frac{1}{2}} U_0 \mathrm{d}X. \tag{6}$$

The dimensionless measured speed is

$$U_M = \frac{u_M}{v_R} = \frac{l}{2v_R}\left(\frac{1}{t_+} - \frac{1}{t_-}\right) = \frac{1}{2M}\left(\frac{1}{T_+} - \frac{1}{T_-}\right) \tag{7}$$

3. FLOW AROUND CYLINDERS AND WAKE MODELS

The fluid flow around circular cross section cylinders has been studied for a long time. The flow has periodic characteristics, which in some cases can be easily appreciated, as the noise generated by a rod moving quickly in the air, or the cables in power distribution lines, or stays. These audible phenomena were systematically studied by the first time by Strouhal, in 1878, which found an approximated relationship $f_c \approx u_\infty/(6d)$ among the frequency of vibrations, f_c, the incoming speed u_∞, and the cylinder diameter, d (Birkhoff 1957). Both the shape and the characteristic frequency of the wake depend on the Reynolds number, as reported in (Schlichting 1979). A brief summary follows: in the range 0 < Re < 4 the flow is dominated by viscous forces, it is attached to the cylinder wall and the streamlines are symmetrical (Stokes' flow). In the range from 4 < Re < 40 the flow remain symmetrical, but the flow is detached, with two big stable vortexes placed in the leeward side of the cylinder. As Re increases, Re > 40, a staggered row of vortexes are alternatively shed from the lateral sides of the cylinder (von Karman´s vortex street). The periodicity of the wake is very stable, and in the range 40 < Re < 10^3, the frequency is given by the Strouhal number S as a function of Re.

$$\mathrm{S} = \frac{f_C\, d}{u_\infty} = 0.21\left(1 - \frac{20}{\mathrm{Re}}\right) \tag{8}$$

For Re > 10^3 the wake starts to appear turbulent, but preserving its periodic character until Re > 10^5.

4. VON KARMAN´S VORTEX STREET CHARACTERISTICS

Based on experimental observations, von Karman developed a mathematical model of the wake of a cylinder, which consists of a pair of staggered rows of an infinite number of vortexes, of opposite sign Γ and $-\Gamma$, the rows placed a distance b of each other, and the centres of the vortexes in each row separated a distance a, as shown in Fig. 3. This simple model describes in a very satisfactory way the phenomenon, and involves only three parameters, Γ, a and b.

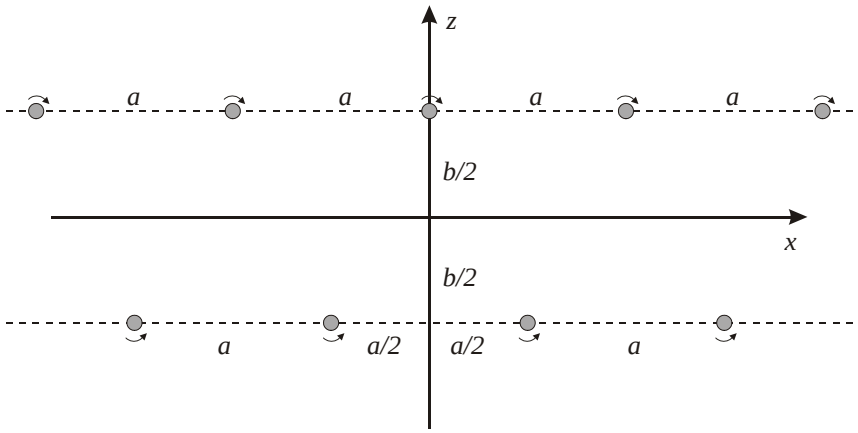

Fig. 3. Von Karman Vortex Street. *b*: separation of vortex rows; *a*: separation between vortexes in each row.

From the potential plane flow theory (Milne-Thomson 1968), it is known that the velocity field generated by a single vortex, placed in the point $\sigma_o = x_o + iz_o$ is derived from a complex potential Q_V

$$Q_V = \mathbf{i}\frac{\Gamma}{2\pi}\ln\left(\sigma - \sigma_0\right) \tag{9}$$

where $\sigma = x + \mathrm{i}z$ represents a point in the complex plane. For a vortex street the complex potential is obtained by addition of the potential of each vortex. In particular, for the vortex street shown in Fig. 3, it is given by:

$$Q_{VS}\left(\sigma\right) = \mathbf{i}\frac{\Gamma}{2\pi}\left\{\ln\left[\sin\left(\frac{\pi}{a}\left(\sigma - \mathbf{i}\frac{b}{2}\right)\right)\right] - \ln\left[\sin\left(\frac{\pi}{a}\left(\sigma - \frac{a}{2} + \mathbf{i}\frac{b}{2}\right)\right)\right]\right\}. \tag{10}$$

Each vortex row induces the same horizontal velocity in each vortex of the other row, in the upstream direction, u_s

$$u_S = \frac{\Gamma}{2a}\tanh\frac{\pi b}{a} \tag{11}$$

The whole vortex street moves at this speed. Therefore, if *a*, *b* and Γ are known, the flow field induced by the vortex street is determined. Then it is necessary to estimate these three parameters as a function of the cylinder diameter, *d*, and the incident velocity, u_∞. From dimensional analysis and experimental data, the following relationships are found:

$$\lambda = \frac{\Gamma}{u_\infty^2}\left(\frac{u_\infty - u_S}{a}\right) \cong 0.2, \qquad \varepsilon = \frac{u_S}{u_\infty} \cong 0.15, \qquad \frac{b}{d} \cong 1.2, \qquad \frac{b}{a} \cong 0.3 \tag{12}$$

These values are used in the following analysis. The reader interested in the details of this development, can consult (Birkhoff 1957).

5. EFFECT OF THE WAKE ON THE MEASUREMENT

Let us consider a wake placed parallel to the measurement path as shown in Fig. 4. The complex potential that represents both the wake and the uniform incoming flow u_∞ is given by

$$Q_{UVS}(\sigma) = u_\infty \sigma + \mathbf{i}\frac{\Gamma}{2\pi}\left\{\ln\left[\sin\left(\frac{\pi}{a}(\sigma-\sigma_{0U})\right)\right]-\ln\left[\sin\left(\frac{\pi}{a}(\sigma-\sigma_{0L})\right)\right]\right\} \tag{13}$$

where σ = (x+iz) = l(X+iZ) is the position in the complex plane, σ_{0U} = ib/2 = i$l$$B$/2, σ_{0L} = a/2 − ib/2 = l(A/2 − iB/2), and

$$A = \frac{a}{l} = \frac{4d}{l} = \frac{4}{\Lambda}, \tag{14}$$

is the dimensionless separation of the vortex, being Λ = l/d the geometric relation of aerodynamic interference that relates the path length, l, with the support diameter, d.

From potential flow theory, the velocity components are

$$u(x,z) = u = \mathrm{Re}\left(\frac{\partial Q}{\partial \sigma}\right), \qquad w(x,z) = w = -\mathrm{Im}\left(\frac{\partial Q}{\partial \sigma}\right) \tag{15}$$

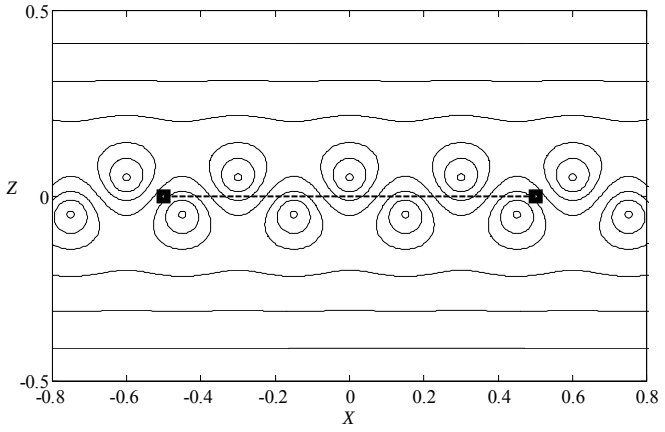

Fig. 4. Streamlines in a von Karman vortex street convected by a uniform flow, parallel to a measurement path P1-P2.

Using dimensionless variables, X = x/l, Z = z/l, reference velocity u_∞, and Eq. (13), the dimensionless velocity components are

$$U = 1 - \frac{\mathrm{K}\,\omega_A}{2}\left\{\frac{\sinh\left[\omega_A\left(Z - B/2\right)\right]}{\cos\left(\omega_A X\right) - \cosh\left[\omega_A\left(Z - B/2\right)\right]} - \right.$$
$$\left. - \frac{\sinh\left[\omega_A\left(Z + B/2\right)\right]}{\cos\left[\omega_A\left(X - A/2\right)\right] - \cosh\left[\omega_A\left(Z + B/2\right)\right]}\right\} \tag{16}$$

$$W = \frac{\mathrm{K}\,\omega_A}{2}\left\{\frac{\sin\left(\omega_A X\right)}{\cos\left(\omega_A X\right) - \cosh\left[\omega_A\left(Z - B/2\right)\right]} - \right.$$
$$\left. - \frac{\sin\left[\omega_A\left(X - A/2\right)\right]}{\cos\left[\omega_A\left(X - A/2\right)\right] - \cosh\left[\omega_A\left(Z + B/2\right)\right]}\right\}, \tag{17}$$

where

$$\mathrm{K} = \frac{\Gamma}{2\pi l u_\infty}; \qquad \omega_A = \frac{2\pi}{A} = \frac{\pi\Lambda}{2} \tag{18}$$

The velocity field is non-rotational at the measurement path, as it is rotational only at the centre of each vortex. The horizontal component at $Z = 0$ could be obtained from Eq. (16) as:

$$U_0 = 1 - \frac{\mathrm{K}\,\omega_A}{2}\left\{-\frac{\sinh\left[\omega_A B/2\right]}{\cos\left(\omega_A X\right) - \cosh\left[\omega_A B/2\right]} \right.$$
$$\left. - \frac{\sinh\left[\omega_A B/2\right]}{\cos\left[\omega_A\left(X - A/2\right)\right] - \cosh\left[\omega_A B/2\right]}\right\}; \tag{19}$$

$$U_0 = 1 + \frac{\lambda}{2\left(1-\varepsilon\right)}\sinh\left(\frac{3\pi}{10}\right)\left\{\left[\cos\left(\frac{\pi\Lambda}{2}X\right) - \cosh\left(\frac{3\pi}{10}\right)\right]^{-1} + \right.$$
$$\left. + \left[\cos\left(\frac{\pi\Lambda}{2}\left(X - \frac{2}{\Lambda}\right)\right) - \cosh\left(\frac{3\pi}{10}\right)\right]^{-1}\right\}, \tag{20}$$

where the definitions of ω_A, A and K have been substituted. After some manipulation Eq. (20) can be reduced to

$$U_0 = 1 + \frac{\lambda}{\left(1-\varepsilon\right)}\frac{\sinh\left(\frac{3\pi}{5}\right)}{\cos\left(\pi\Lambda X\right) - \cosh\left(\frac{3\pi}{5}\right)} \tag{21}$$

Before computing and analysing the measured velocity $U_M = \overline{U_0}$, let briefly analyse the behaviour of U_0 along the measurement path. Note that U_0 depends on X with $\Lambda = l/d$ as a parameter. This variation is shown in Fig. 5. Note that U_0 is always $U_0 < 1$, as the velocity generated at the measurement path by the vortex street is negative (opposed to u_∞, used as reference). U_0 is a periodic function of X, whose amplitude (independent of Λ) is obtained from Eq. (21) taking into account that the extreme values appear at $X = X_m$ fulfilling the condition $\cos(\pi\Lambda X_m) = \pm 1$, that is, $0.36 < U_0 < 0.65$. The minimum values appear just at the same longitudinal position of the vortexes, and the maximum values in the middle.

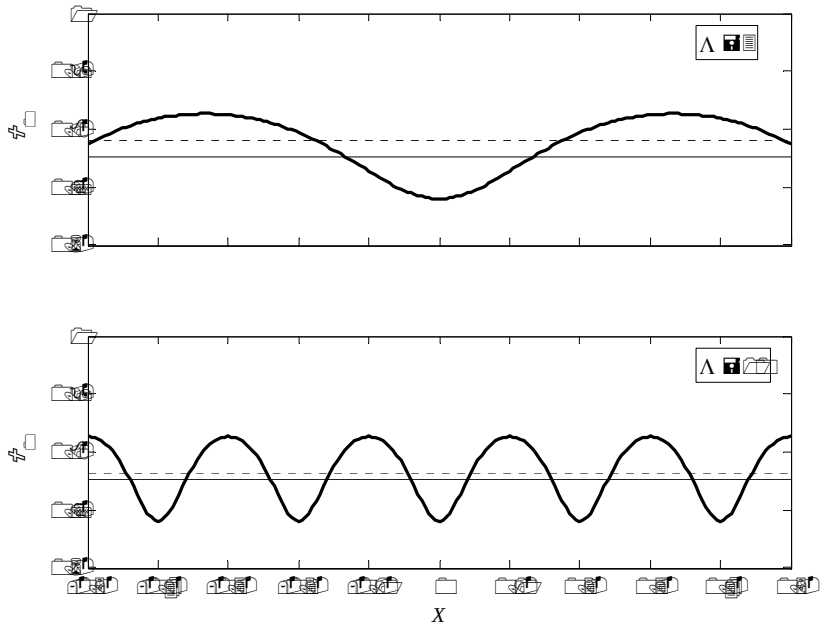

Fig. 5. Variation of the horizontal velocity component U_0 with the position along the measurement path, X (solid line). Aerodynamic interference parameter, $\Lambda = l/d$. Mean value (dotted line).

From Eq. (21), the central value corresponds to $U_{0C} = U_0(X_c)$ such as $\cos(\pi\Lambda X_c) = 0$

$$U_{0C} = 1 - \frac{\lambda}{(1-\varepsilon)} \coth\left(\frac{3\pi}{5}\right) = 0.7536, \tag{22}$$

which is displayed in Fig. 5 as a dashed horizontal line. It is different from the average value $\overline{U_0}$ (dotted line), because of the lack of symmetry of the cycle with regard to the central value. On the other hand, the period of the oscillations ΔX depends on the aerodynamic interference geometric parameter Λ, and is obtained from the condition

$$\pi\Lambda\Delta X = 2\pi, \tag{23}$$

that is

$$\Delta X = \frac{2}{\Lambda}. \tag{24}$$

Note that increasing Λ means increasing the length of the measurement path, and therefore the number of vortexes present in the space between the two transducers of the measurement path ($1/2 \leq X \leq 1/2$). This situation implies that the measured speed $\overline{U_0}$ will depend on the number of cycles included in the measurement path. If N_C is the number of cycles inside the measurement path ($-1/2 < X < 1/2$) then

$$N_C = \frac{1}{\Delta X} = \frac{\Lambda}{2} \tag{25}$$

Following the same approach in (Franchini 2007), the acoustic pulse trajectory is considered a straight line and, neglecting M^2 order terms, the measured speed U_M is obtained as $U_M = \overline{U_0}$. So, the measured speed U_M is given by

$$U_M = \overline{U_0} = \int_{-\frac{1}{2}}^{\frac{1}{2}} U_0 \mathrm{d}X; \tag{26}$$

The analytical result is too complex to be useful, so that a numerical solution of Eq. (26) has been employed to obtain the results shown in Fig. 6, where the deviation of velocity $H = U_M - 1$ is plotted as function of the aerodynamic interference parameter Λ for a wake in the position $X_{t0} = 0$ shown in Fig. 3.

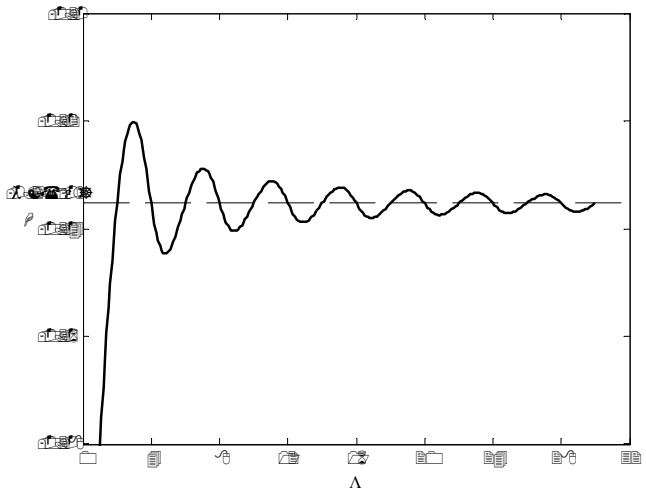

Fig. 6. Variation of the velocity deviation, H, generated by a vortex street, with the aerodynamic interference parameter, $\Lambda = l/d$.

The period of the curve $H(\Lambda)$, $\Delta\Lambda = 4$, comes from the separation of the vortexes in the wake $a = 4d$, which in dimensionless form is $A = 4/\Lambda$. Therefore, the number of vortex in a row, inside the measurement path, is $l/a = 1/A = \Lambda/4$. So that, as Λ increases each time Λ coincides with a multiple of 4 a new vortex is included inside the measurement path. Remember that the effect of a vortex placed downstream of the second transducer is negligible. The central value of H is obtained at the middle and at the extremes of each cycle (except the first one). Observe in Fig. 5 that the period of the U_0 is half the distance between two consecutive vortexes ($A/2 = 2/\Lambda$), whereas the period of the H cycle is $\Delta\Lambda = 4$.

Note that a new cycle starts each time the effect of a new vortex is included in the measurement path. However the distance between two vortexes (cycle H) includes two U_0 cycles, because the vortexes in the opposite row should be also considered. On the other hand, the amplitude of H cycle decreases as Λ increases, because of the increasing number of vortexes included in the measurement path, which minimizes the effect of each new vortex. The curve approaches asymptotically to the value $-\lambda/(1-\varepsilon) = 0.23$. This behaviour is similar to the "leakage" effect that appears when a periodic signal is sampled at a rate that is not a multiple of the signal period.

As an example, in Table 1 the characteristic dimensions and the values of H are shown, for the two commercial anemometers. Observe that the effect is significant in both cases.

Table 1. Characteristic dimensions and measured velocity deviation induced by interference of a wake, whose configuration corresponds to that shown in Fig. 4.

Anemometer	**d×10^{-3} [m]**	**l×10^{-3} [m]**	**Λ**	**H×10^{2}**
WindMaster	6	145	24.17	–23.6
USA-1	9	173	19.22	–23.3

5.1. Block average (moving wake)

The results obtained in the previous section apply to the case where only one measurement is made, that is, it seems that the vortex street remains fixed. However, in a real situation, the most often used procedure in commercial applications is based on the average of a set of consecutive N_B measurements. In this case the vortex street will change its position in the time interval from one measurement to the following one, and therefore the influence in each measurement will be different.

The wake moves downstream parallel to itself, under the effect of both the incoming flow, u_∞, and its self-induced speed, u_S, so that the total speed of the wake displacement is $u_{VS} = u_\infty - u_S$. Therefore, the wake changes its position during the sampling interval, which has an impact on the measurements and on the average value. The complex potential is the same as in the previous section, but now the position of the vortexes change, to take into account their displacement, that is

$$\sigma_{0\mathrm{U}} = l\left[\left(X_{t0} + \frac{u_{VS}t}{l}\right) + \mathbf{i}\frac{B}{2}\right], \qquad \sigma_{0\mathrm{L}} = l\left[\left(X_{t0} + \frac{A}{2} + \frac{u_{VS}t}{l}\right) - \mathbf{i}\frac{B}{2}\right], \tag{27}$$

where X_{t0} is the reference position of the wake at the start of measurements, $t = 0$. $X_{t0} = 0$ is the configuration shown in Fig. 4. The value of the horizontal velocity component along the measurement path ($Z = 0$), U_0 is given by

$$U_0 = 1 + \frac{\lambda}{(1-\varepsilon)} \frac{\sinh\left(\frac{3\pi}{5}\right)}{\cos\left\{\pi\Lambda\left[X - \left(X_{t0} + \frac{u_{VS}}{l}t\right)\right]\right\} - \cosh\left(\frac{3\pi}{5}\right)}, \tag{28}$$

where "t" is the sampling time. In order to perform the block average of N_B consecutive measurements sampled at frequency f_S , the sampling time can be written as $t = (i - 1)/f_S$ ($i = 1, 2\ldots, N_B$) and a general expression for the velocity field along the measurement path, just at the "i" sample, can be obtained

$$U_0(i) = 1 + \frac{\lambda}{(1-\varepsilon)} \frac{\sinh\left(\frac{3\pi}{5}\right)}{\cos\left\{\pi\Lambda\left[X - \left(X_{t0} + (1-\varepsilon)(i-1)L_S\right)\right]\right\} - \cosh\left(\frac{3\pi}{5}\right)}, \tag{29}$$

where $L_S = u_\infty/(f_S l)$ is the dimensionless sampling interval. In Eq. (29) the relation $u_S = \varepsilon u_\infty$ has been substituted. This expression is like Eq. (21) for a static wake, but now the argument of the cosine function includes a phase angle that depends on the parameters X_{t0}, i, Λ, ε and L_S.

The general expression for the velocity measured at a given instant i is $U_M(i) = 1 + H(i)$, where

$$H(i) = \frac{\lambda}{(1-\varepsilon)} \frac{\sinh\left(\frac{3\pi}{5}\right)}{\cos\left\{\pi\Lambda\left[X - \left(X_{t0} + (1-\varepsilon)(i-1)L_S\right)\right]\right\} - \cosh\left(\frac{3\pi}{5}\right)}. \tag{30}$$

The velocity obtained from the block average, referred to u_∞ is defined as

$$U_B = \frac{u_B}{u_\infty} = \frac{1}{N_B}\sum_{i=1}^{N_B} U_M(i) = 1 + \frac{1}{N_B}\sum_{i=1}^{N_B} H(i) = 1 + H_B. \tag{31}$$

The term H_B is the average of the deviations generated by the vortex street wake at each one of the N_B samples. The aim of the averaging is to reduce as much as possible the distortion of the measurement generated by the wake. Then, the averaged deviation is given by

$$H_B = \frac{1}{N_B}\sum_{i=1}^{N_B} H(i), \tag{32}$$

where $H(i) = U_M(i) - 1$ is the deviation of each single measurement and $U_M(i)$ is obtained from Eq. (26) with $U_0(i)$ given by Eq. (29).

The integration and summation needed to obtain the results are carried out numerically. The average deviation H_B is a function $H_B = H_B(\Lambda, N_B, L_S, X_{t0})$ which shows the dependence of H_B on the aerodynamic interference parameter $\Lambda = l/d$, on the position of the wake at the sampling start time $t = 0$ through the parameter X_{t0}, on the dimensionless sampling time L_S, and on the number of samples N_B. The effect of each parameter is analysed below. The variation of H_B as a function of Λ for several values of X_{t0} and $N_B = 1$ is shown in Fig. 7. Obviously these results are like the ones obtained for a static wake (because $N_B = 1$), the effect of X_{t0} is not relevant, and H_B decreases as Λ (that is, the number of vortexes in the measurement path) increases. The amplitude of the oscillations does not depend on X_{t0}, and the mean value is the same $H_B = -\lambda/(1-\varepsilon) = -0.23$ as above mentioned. However a number of new harmonics appears when $X_{t0} \neq 0$, due to the rupture of the symmetry of the wake with regard to the centre of the measurement path, although the basic period $\Delta\Lambda = 4$ is preserved, and it is $H_B = -\lambda/(1-\varepsilon)$ not only for $\Lambda = 2K$ ($K = 1,2\ldots$), as in the case $X_{t0}=0$, but also in some intermediate points.

Concerning the effect of the aerodynamic interference parameter Λ, the variation of H_B for several values of N_B and of the sampling interval L_S is shown in Fig. 8 for $X_{t0} = 0$.

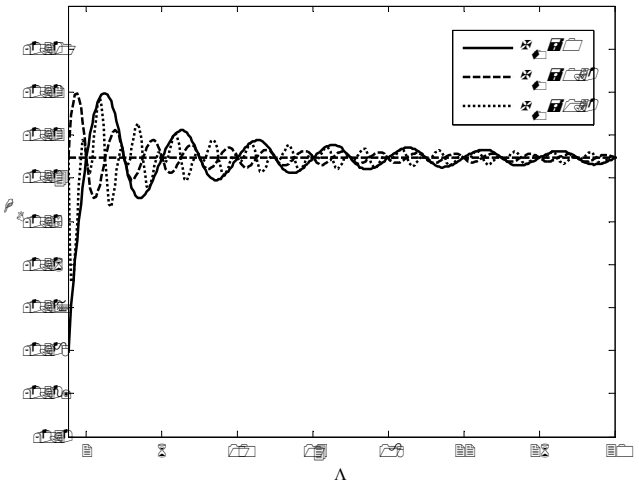

Fig. 7. Variation of the averaged velocity deviation, H_B, generated by a vortex street, with the aerodynamic interference parameter, Λ. X_{t0} is the initial position. Only one sample is considered, $N_B = 1$.

As was above mentioned, as Λ or N_B increases, the effect of the averaging smoothes out the influence of the new vortex that appears in the measurement path

each time Λ increases a quantity $\Delta\Lambda = 4$. H_B oscillates around the central value $-\lambda(1-\varepsilon)$, although the amplitude decreases with both Λ and N_B. The effect of increasing the number of samples and the displacement of the vortexes between samples, $L_{S,}$ is to include some harmonics, which are due to the angle phase changes produced by L_S and "*i*" in the argument of cosine function in Eq.(29). In spite of the presence of these new harmonics, H_B shows the characteristic periodic behaviour with period $\Delta\Lambda = 4$, crossing through $H_B = -\lambda(1-\varepsilon) = -0.23$ at least when Λ is an even number. Therefore, the wake induces a deviation of the measured speed which is close to 20% of the free stream value.

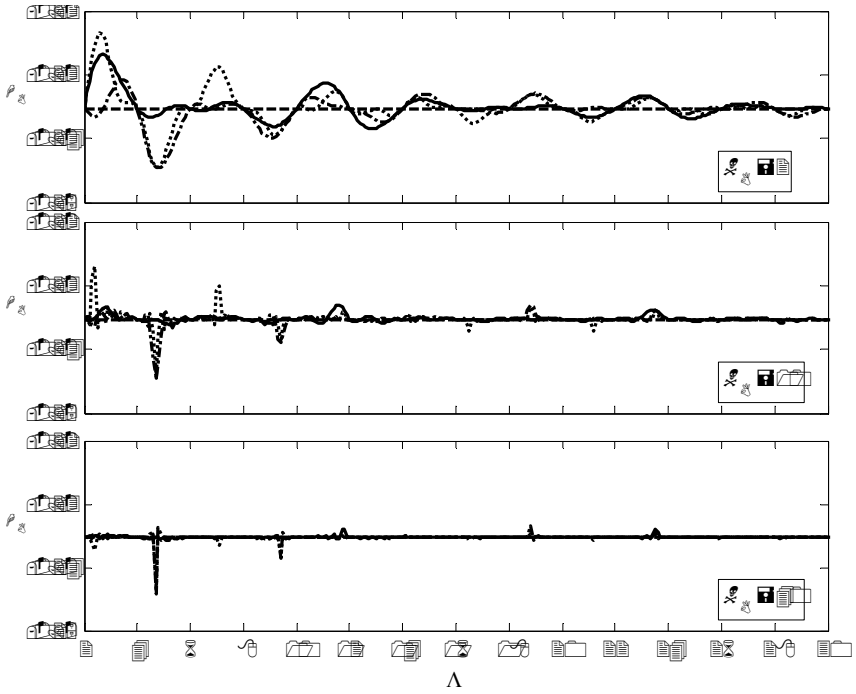

Fig. 8. Variation of the averaged velocity deviation, H_B, generated by a vortex street, with the aerodynamic interference parameter, Λ. L_s is the dimensionless sample interval: 0.2 (solid line), 0.5 (dot-dashed line), 1 (dotted line).

6. VALIDATION OF THE MODEL

In order to validate the presented model, a preliminary wind tunnel test has been performed on a single path UA. This single path is a modification of a SATI Ultrasonic Anemometer/Thermometer from Applied Technologies, Inc. especially developed for research (see Fig. 9).

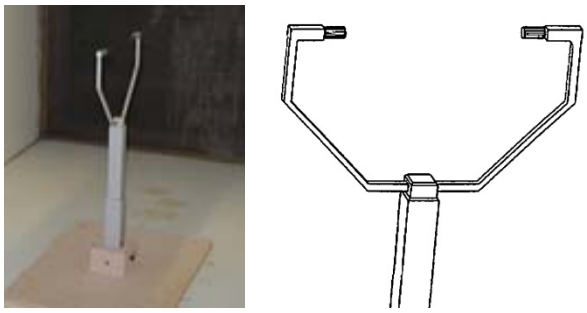

Fig. 9. Single path ultrasonic anemometer especially developed for research, a Modification of a SATI Ultrasonic Anemometer/Thermometer from Applied Technologies, Inc.

The supports of this UA have been modified in order to reproduce the conditions of the theoretical model. Two cylinders of acrylic and 5×10^{-2} m diameter have been fixed around the transducers in such a way that the the geometric relation of aerodynamic interference is $\Lambda = l/d = 3$. Fig. 10 shows a scheme of this configuration.

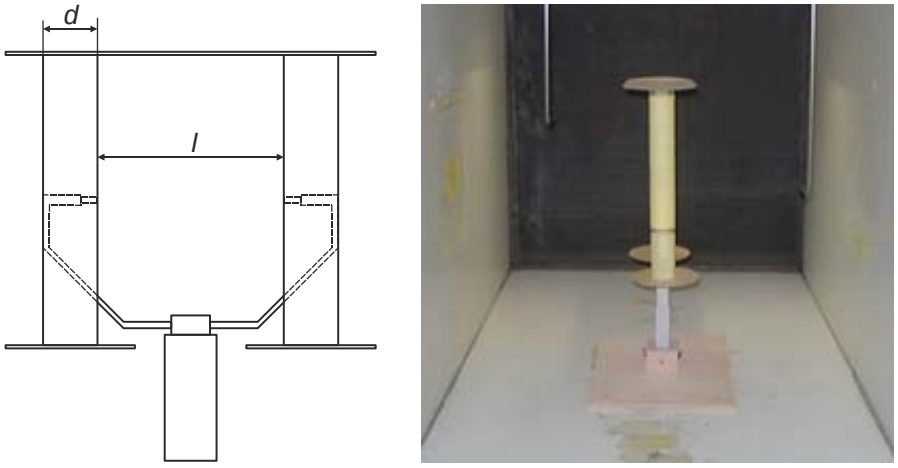

Fig. 10. Right: A scheme of the modified support of a single path ultrasonic anemometer. Left: the model installed in the wind tunnel test chamber.

The experiments were performed at the S4C wind tunnel at the Instituto Universitario “Ignacio Da Riva” of the Universidad Politécnica de Madrid (IDR/UPM). This facility is an open-circuit wind tunnel having a closed square test section of 0.9 m

side. The maximum attainable speed in the test section is nearly 23 m/s with a flow uniformity under 0.2% in the testing area.

The modified ultrasonic anemometer was fixed to the wind tunnel floor, with the sonic path aligned with the main flow. During the test the wind velocity has been varied between 5 m/s to 15 m/s. Once the wind tunnel reaches it steady state condition, the output of the ultrasonic anemometer was acquired at a sampling frequency fs = 50 Hz and taking 2100 samples. The wind speed in the testing chamber is measured by an Airfl ow 0.48 Pitot (AIRFLOW Instruments, TSI Instruments Ltd.: Buckinghamshire, UK) tube connected to a Druck LPM 9481 (GE Sensing: Billerica, MA, USA) high-precision pressure transducer. Temperature and humidity sensors (Vaisala PTU 200 and Vaisala HMP45D) are used to determine the air density value.

With this data, the average of the velocity deviation, H_B, has been determined. Fig. 11 show the variation of H_B with the dimensionless sampling interval, $L_S = u_\infty/(f_S l)$.

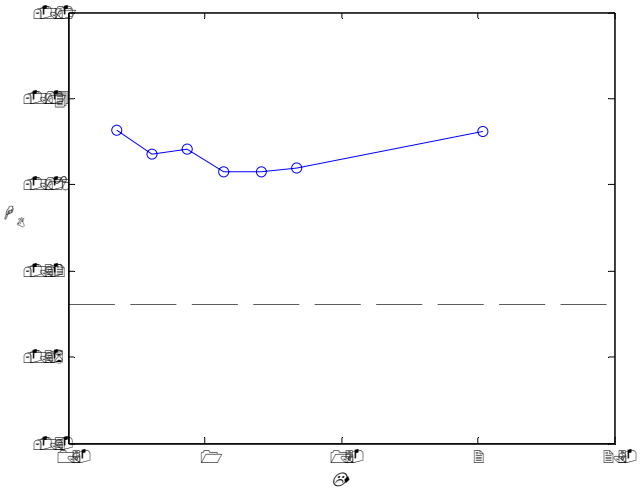

Fig. 11. The variation of the average of the velocity deviation, H_B, with the dimensionless sampling interval, $L_S = u_\infty/(f_S l)$.

This experimental data shows that the average of the velocity deviation determined is approximately constant, being $H_B \approx -0.16$. For the same conditions of the wind tunnel test, the theoretical model here presented predict an average of the velocity deviation H_B = -0.23. The difference is because the Reynolds number based in the cylinder diameter is about 10^4, so, although the wake still preserving its periodic character, the diffusivity of turbulence disturbs the vortex street structure.Taking in account this fact, it can be considered that there are good agreements between experimental and theoretical.

At the time of writing this report, a new set of test are being performed, but with smaller wind speeds, in order to obtain Reynolds numbers in the order of 10^3 and produce a vortex street wake. In this test, the reference wind speed is measured with hot wire anemometry, so that it is possible to measure small values of wind speed with a small uncertainty.

7. CONCLUSIONS

In this paper the effect of the wakes of the supports on the measured velocity has been modelled in a simplified way and analysed. The effect of a vortex wake has been considered on both a single measurement, and on the average of a set of measurement. The von Karman's vortex street has been employed as wake model. Typical values of the vortex street parameters have been employed.

It has been found that the velocity component along the measurement path changes in a periodic way along the path (with a period half the separation of the vortexes in a row of the street). As the deviation is produced by the average of the velocity along the measurement path, the number of cycles considered in the average is relevant. If the number of cycles is a natural number, the mean value is obtained, although, if it is not, a "leakage" effect appears, because a fraction of a cycle is included in the averaging process, contributing to the mean value. Therefore, an oscillation of the deviation around the asymptotic mean value appears whose amplitude decreases as the number of cycles considered in the averaging increases.

The mean value of the deviation, some -0.23, seems to be too high for an actual anemometer, but consider that the configuration studied corresponds to an extreme situation where the measurement path is placed completely inside the wake of a rod. In a practical case, the orientation of the measurement paths with regard to the supporting rods is not so unfavourable, and the velocity deviation should be smaller. The calculation of the deviation for a given anemometer model would require a dedicated study, taking into account the section of the measurement path which is crossed by the wake.

The effect of the longitudinal position of the wake (X_{t0}), relative to the measurement path does not seem to have a relevant influence. Concerning the effect of averaging several individual measurements, the amplitude of the oscillations around the mean value decreases, appearing only some individual peaks at some given dimensionless measurement path length, Λ (Fig. 8).

The comparison with the experimental data is reasonable good. It should be outlined that the comparison is not strictly valid because the experimental configurations are different from the configuration considered in the theoretical model. More experiments are needed at a low Reynolds numbers in order to obtain conditions more close to the ones considered in the theoretical model.

8. ACKNOWLEDGE

The work presented in this article is part of the AUM project, which is financed by the Ministry of Science and Innovation of Spain (Ministerio de Ciencia e Innovación, project reference: ENE2009-10670).

9. REFERENCES

Birkhoff G., Zarantonello E.H. (1957), *Jets, wakes and cavities*, Academic Press.

Cuerva, A., Sanz–Andrés, A. and López García, O. (2004), "Singularities and Undefinitions in the Calibration Functions of Sonic Anemometers", J. Atmos. Ocean. Technol., vol. 21, 1868–1875.

Franchini, S., Sanz–Andrés, A., and Cuerva, A. (2007), “Effect of the Pulse Trajectory on Ultrasonic Fluid Velocity Measurement,” Exp Fluids, vol. 43, Num. 6, 969–978.

Kaimal, J.C. (1978), “Sonic Anemometer Measurement of Atmospheric Turbulence” Dynamic Flow Conference, Pergamon Press, 551–565.

Milne-Thomson L. M. (1968), *Theoretical Hydrodynamics*, MacMillan.

Schlichting H. (1979), *Boundary-Layer Theory*, Seventh Edition, McGraw-Hill.

Wyngaard, J. (1985), “Transducer–Shadow Effects on Turbulence Spectra Measured by Sonic Anemometers”, J. Atmos. Ocean. Technol., vol. 2, 548–558.